SLAC-PUB-2395
September 1979
(T/E)

NUCLEAR PHENOMENA AND THE SHORT DISTANCE STRUCTURE OF HADRONS*

Stanley J. Brodsky
Stanford Linear Accelerator Center
Stanford University, Stanford, California 94305

ABSTRACT

In certain cases, nuclear corrections to hadronic phenomena depend in detail on the nature of quark and gluon interactions, as well as the effects of jet development within the nuclear medium. In this talk I review applications of quantum chromodynamics to fast particle production in nuclear collisions, nuclear form factors, and shadowing in deep inelastic lepton processes. I also discuss a new approach to particle production in hadron-nucleus, nucleus-nucleus and deep-inelastic nuclear reactions from the standpoint of a color-neutralization model.

(Invited talk presented at the First Workshop on Ultra-Relativistic Nuclear Collisions, Berkeley, California, May 21-24, 1979.)

---

* Work supported by the Department of Energy under contract number DE-AC03-76SF00515.

I. Introduction

A basic premise of this workshop is that there are aspects of hadronic physics which can only be studied in nuclear collisions. The most dramatic possibility is that novel collective hadronic degrees of freedom or a new phase of hadronic matter will be initiated in central, high-energy heavy-ion collisions.[1] Even if this turns out not to be the case, one can argue that the nucleus is an essential tool for the study of fundamental hadronic mechanisms at distances where the quark and gluon degrees of freedom are relevant.[2]

In this talk I will discuss several topics involving nuclear collisions where one can possibly test and study interesting aspects of quantum chromodynamics (QCD). These include

(A) Hadronic production in hadron-nucleus, lepton-nucleus and nucleus-nucleus collisions.

(B) The question of shadowing in deep inelastic nuclear reactions.

(C) The structure of the nuclear wave function at very short distances and nuclear form factors.

Of course, the advantage of being able to study hadronic mechanisms in close proximity to other quarks and gluons in nuclei has to be counterbalanced by the complexity of the nucleus. By turning to nucleus-nucleus collisions we exactly reverse Feynman's famous analog,[3] in which he compares proton-proton collisions to the smashing together of two delicate watches; it is obviously much simpler to study elementary "gear-gear" interactions, as in e^+e^- collisions. The nucleus-nucleus collision seems to be the analog of the collision of two grandfather clocks, or perhaps

even whole jewelry stores! Despite this, there are fascinating, controversial questions concerning the physics of nuclear collisions which appear to depend in detail on basic mechanisms at the quark and gluon level. This talk touches on only a fraction of these problems, but I hope it will serve to stimulate further experimental and theoretical studies.

II. Hadron Production in Nuclear Collisions

There is now extensive data on hadron production in nuclei from meson, baryon, and lepton beams at laboratory energies up to 200 GeV.[4] The subject is fascinating to theorists, but there is little concensus on the basic particle production mechanisms within the nucleus. This is understandable, since it is not clear we even understand particle production in ordinary nucleon-nucleon collisions! The simplest particle production model consistent with the framework of QCD is the gluon-exchange model of Low[5] and Nussinov.[6]

Let us suppose that two protons interact by the exchange of a single soft gluon (a color octet). This leaves the spectator quarks in each nucleon excited as color octets [see Fig. 1(a)]. The subsequent color neutralization of these two "jets" and the recombination of the gluons and quarks into hadrons is evidentally similar to the particle production mechanism which occurs in $e^+e^- \to q\bar{q} \to$ hadrons.[7] This picture is obviously oversimplified, however in analogy with QED it predicts[7] (a) a uniform central rapidity distribution — expanding as log s (due to the spin-one nature of the gluon) [see Fig. 1(b)], (b) a transverse momentum cutoff (due to hadronic wave function fall-off), (c) a multiplicity distribution

which rises faster than log s (similar to analogous effects in soft photon radiation in QED), and (d) a nearly constant total cross section which depends on the color dipole moment, and hence the size and quark content of the interacting hadrons.

In effect this color-neutralization model leads to final states not so different from the standard multiperipheral model productions, but the underlying mechanisms and time sequence are quite different.

Let us now consider the implications of this picture for a hadron-nuclear collision. Figure 2 illustrates an event where a gluon is exchanged between an incident hadron H and a nucleon N_1 in nucleus A. The quarks and gluons produced in the color-neutralization can subsequently interact and color-excite further nucleons; the figures represents an event where $\nu = 3$ nucleons in A are "wounded." For the average number of wounded nucleons we can use the standard geometrical estimate $\bar{\nu} = A\sigma_{HN}^{inel}/\sigma_{HA}^{inel}$. For simplicity we will first consider the case where one quark of H (and its neutralization cloud) interacts; multiquark interactions will be taken into account later.

The expected multiplicity distribution corresponding to the $\nu = 3$ event of Fig. 2 is shown in Fig. 3(a). We plot the ratio $R_{HA}(y) = [dN/dy]_{HA}/[dN/dy]_{HN}$ (the multiplicity distribution normalized to nucleon-target data) in order to isolate the nuclear effects. The multiplicity distribution ratio for $y < y_A$ reflects the wounding of $\nu = 3$ quarks: $R_{HA}(y) = \nu$. The multiplicity for $y > y_H$ in the projectile region in the simple model is $R_{HA}(y) = 1$; a more detailed model which allows for multi-quark interactions would give $R_{HA}(y) < 1$, reflecting energy-momentum loss. Our analysis here will closely follow the formulation of Ref. (8).

Let us now assume that the rapidity of any of the secondary quarks or gluons which excite N_2 and N_3 in Fig. 2 occur — on the average — uniformly in rapidity in the central region. (This simple assumption is in fact controversial since it can be argued that the fast constituents produced in the first neutralization tend to be produced outside the nuclear volume. This would bias the secondary interactions toward target rapidities.[9]) Averaging over events then gives the "ramp"-like distribution ratio $R_{HA}(y)$ shown in Fig. 3(b). Analytically, one finds for $y_A < y < y_H$,[8]

$$R_{HA}(y) = \bar{\nu}\left[1 - \left(\frac{y - y_A}{y_C}\right)\right] + \left[1 - \left(\frac{y_H - y}{y_C}\right)^{\bar{\nu}}\right] \qquad (2.1)$$

where $y_C = y_H - y_A \sim \log s$ is the length of the central region. The first term in (2.1) represents the hadrons produced from the $\bar{\nu}$ nuclear excitations. The second term represents the multiplicity produced by the repeated excitation of H and its products. Integrating over the central region gives the ratio,

$$R_{HA} = \frac{N_{HA}}{N_{HN}} = \frac{\bar{\nu}}{2} + \frac{\bar{\nu}}{\bar{\nu}+1} \qquad \left(y_A < y < y_H\right) \qquad (2.2)$$

(The second term $\bar{\nu}/(\bar{\nu}+1)$ gives the mean fraction of the central region populated by H and its products.) Including the fragmentation regions

$$R_{HA} = \left(\frac{\bar{\nu}}{2} + \frac{\bar{\nu}}{\bar{\nu}+1}\right)\frac{\langle n_{CENTRAL}\rangle_{HN}}{\langle n_{TOT}\rangle_{HN}} + \bar{\nu}\,\frac{\langle n_{FRAG}\rangle_{N}}{\langle n_{TOT}\rangle_{HN}} + \frac{\langle n_{FRAG}\rangle_{H}}{\langle n_{TOT}\rangle_{HN}} \qquad (2.3)$$

where $\langle n_{TOT}\rangle_{HN} = \langle n_{CENTRAL}\rangle_{HN} + \langle n_{FRAG}\rangle_{N} + \langle n_{FRAG}\rangle_{N}$. Thus

$$\left(\frac{\bar{\nu}}{2}+\frac{1}{2}\right) \leq R_{HA} \leq \left(\frac{\bar{\nu}}{2}+\frac{\bar{\nu}}{\bar{\nu}+1}\right) \qquad (2.4)$$

where the upper limit is reached for $s \to \infty$. Note that R_{HA} only depends on the projectile cross section through $\bar{\nu} = A\sigma_{HA}^{inel}/\sigma_{HN}^{inel}$. A comparison of this simple prediction with the data of W. Busza et al.[10] is shown in Fig. 4(a). The prediction given in Eq. (2.1) also gives a good representation of the 200 GeV p-A (pseudo-rapidity) data of Azimov et al.[11] in the central region [see Fig. 4(b)]. For $y > y_H$, the data shows that $R_{HA} < 1$, indicating energy-momentum losses for the fast fragments of H; for $y < y_A$ there are indications of cascading in the nuclear target fragmentation region, at least for heavy nuclei.

Let us now turn to nucleus-nucleus collisions $B + A \to X$, and consider the multiplicity ratio (normalized to nucleon-nucleon collisions)

$$R_{BA}(y) = \frac{dN/dy\ (B+A \to X)}{dN/dy\ (N+N \to X)} \qquad (2.5)$$

In virtually all models one expects the ratio in the fragmentation regions ($y \lesssim y_A$, $y \gtrsim y_B$) to equal the number of wounded constituents (nucleons), $W_A = A\sigma_{NB}/\sigma_{AB}$, and $W_B = B\sigma_{NA}/\sigma_{AB}$ in A and B respectively. The interesting question is what $R_{BA}(y)$ looks like in the central region. Several very different possibilities are implies by models in the literature [see Fig. 5(b)]. In the Reggeon-calculus multiple-cut model of Ref. 12, independent (multiperipheral model) chains contained within the projectile wave function are excited and produce multiplicity throughout the central region (subject to overall energy conservation). In the early parton-model approach of Ref. 13, the multiplicity produced due to nuclear excitation occurs only locally in the nuclear target fragmentation region.

The quark-constituent model of Ref. 14 leads to a "3-step" picture since only flat plateau regions are allowed. In the color-neutralization model discussed here, there is no such constraint and the central region smoothly interpolates between the two fragmentation regions.

The calculation of the multiplicity ratio in the color-neutralization model for nucleus-nucleus collisions $A+B \to X$ is only slightly more complicated than the nucleus-nucleus case. Notice that each nucleon of A can potentially break-up any nucleon of nucleus B. The average number of times each nucleon in A interacts in B is $\bar{\nu}_B = B\sigma_{NN}^{inel}/\sigma_{BN}^{inel}$. We then find:[8]

$$R_{BA}(y) = \frac{dN/dy\ (B+A)}{dN/dy\ (N+N)} = W_A\left[1-\left(\frac{y-y_A}{y_C}\right)^{\bar{\nu}_B}\right] + W_B\left[1-\left(\frac{y_B-y}{y_C}\right)^{\bar{\nu}_B}\right] \tag{2.6}$$

and the integrated ratio in the central region is

$$R_{BA} \equiv \frac{\langle n\rangle_{B+A}}{\langle n\rangle_{N+N}} = W_A\left[1-\frac{1}{\bar{\nu}_B+1}\right] + W_B\left[1-\frac{1}{\bar{\nu}_A+1}\right] \tag{2.7}$$

There is very little data for nuclear-nuclear collisions. One example is $R_{BA} \cong 3.8$ for $\alpha+A$, $A > 100$ from Eq. (2.7) compared to a ratio of order ~4 from cosmic rays.[15] A comparison of Eq. (2.7) with the model of Bialas, Czyz and Furmanski[14] is shown in Fig. 6. We also note that for $y_{cm}=0$, Eq. (2.6) predicts

$$\frac{W_A+W_B}{2} \le R_{AB}\ (y_{cm}=0) \le W_A+W_B \quad ; \tag{2.8}$$

the ratio is maximal at $y_{cm}=0$ if $A=B$.

Having worked out the nucleus-nucleus case, it is simple to generalize the model and allow any or all of the quarks of each nucleon to interact; we simply count "wounded" and interacting quarks rather than nucleons. For example, we can apply Eqs. (2.6) and (2.7) to N-N collisions, taking each nucleon as a "nucleus" with 3 quarks; then

$$W_N = 3\sigma_{qN}/\sigma_{NN} \geq 1 \tag{2.9}$$

and

$$\bar{\nu}_q = 3\sigma_{qq}/\sigma_{qN} \geq 1 \tag{2.10}$$

giving the ratio

$$\frac{dN/dy\ (p+p)}{dN/dy\ (q+q)} = W_N\left[1 - \left(\frac{y - y_A}{y_C}\right)^{\bar{\nu}_q} + 1 - \left(\frac{y_B - y}{y_C}\right)^{\bar{\nu}_q}\right] \tag{2.11}$$

An amusing feature of this result is that $dN/dy(p+p)$ has a bowed distribution, maximal at $y_{cm} = 0$ even if $dN/dy(q+q)$ is flat. This also predicts that $dN/dy(\pi - N)$ is less bowed but is slightly asymmetrical about $y_{cm} = 0$. The previous results for $R_{HA}(y)$ and $R_{AB}(y)$ are unchanged if $\sigma_{qN} = \frac{1}{3}\sigma_{NN}$, $\sigma_{qq} = \frac{1}{3}\sigma_{qN}$ (since they are normalized to N-N collisions); thus one only expects minor changes for the multiplicity ratios for nuclei even if the quark cross sections are screened.

In order to justify the simple counting of quarks as constituents in inelastic reactions, let us consider a meson-nucleus collision where both the quark and antiquark each exchange a color gluon with the target [see Fig. 7]. After two soft gluon-exchanges, the $q\bar{q}$ system can be in either a color octet or color singlet state. If we assume that the resulting hadronic multiplicity is proportional to the color charge (Casimir operators 9/4 and 0 respectively), then the statistical average

over events gives

$$\frac{dN}{dy} \propto \left(\frac{8}{9}\right) \times \left(\frac{9}{4}\right) + \left(\frac{1}{9}\right) \times (0) = 2 \qquad (2.12)$$

i.e., the same result as an incoherent sum. Nevertheless, color coherence implies that the multiplicity distribution will have large fluctuations about the mean.

It is interesting to apply the color neutralization model to deep inelastic lepton scattering on a nuclear target [see Fig. 8]. For large Q^2, the interaction begins with the scattering of a quark in the target along the virtual γ (or W) direction. The particles produced in the color-neutralization of the separated q and qq then can interact and excite additional nucleons in the nucleus.[16] Thus, even though the observed cross section is linear in the nucleon number A, several nucleons can be "wounded" in the deep inelastic process. These expectations can be compared with the inelastic p_{lab} = 150 GeV/c muon-emulsion data shown in Fig. 9(a) from the Cornell, FNAL, Cracow collaboration.[17] The shape of the multiplicity distribution (in pseudo-rapidity η) for incident 150 GeV μ^+ is not very dissimilar from corresponding 60 GeV/c pion-emulsion data! The magnitude of the produced multiplicity in the central region is not quite as large as the pion induced multiplicity, but the data in Fig. 9(b) shows that mean total multiplicity in deep inelastic muon-emulsion collisions is much larger than the corresponding μ-p multiplicity, independent of the value of $\omega = 2q\cdot p/Q^2$. These results give strong evidence that the energy associated with "quark jet" production is effective in producing hadrons in its passage through the nucleus. The similar shapes for dN/dy for μp and πp gives support to the idea that

the same color-neutralization mechanisms are effective in both processes. Further study of particles produced in deep inelastic processes in heavy nuclei, especially the Drell-Yan reaction, $H + A \to \mu^+\mu^- X$, is clearly very important for understanding the basic interactions of q and qq jets in the nuclear medium.

The color-neutralization model presented here, though simple, is based on QCD and should give a reasonable guess on what happens in nucleus-nucleus collisions if such mechanisms are relevant. Although I have done a complete analysis, I believe that this color approach is consistent with generalized Glauber theory; the hadronic multiplicity can be computed from unitarity cuts of the forward scattering amplitude.

In principle, there could be mechanisms operating in high energy nucleus-nucleus collisions which would not occur in hadron-nucleus collisions. For example, the color neutralization of many jets in a single collision could lead to some type of anomalous phenomena, such as an overall excitation or "heating" of the nuclear system. The observables include $dN/dy(A_1 + A_2)$, the π/K ratio, charm production, leading particle production, the associated multiplicity in massive lepton pair (on and off resonance), and the rate of η or ψ production or direct photon[18] production, as a hint of anomalous gluon production. I should emphasize that the analysis presented here is only semi-qualitative. However, the basic formulation and results are so simple that they may well be useful as a guide and parametrization of the data.

III. Shadowing in Deep Inelastic Lepton Scattering on Nuclei

It is well known that the photoabsorption cross section for on-shell photons on nuclei at SLAC[19] and Cornell[20] energies is not additive in the nuclear number; empirically $\sigma_{\gamma A} \sim A_{eff}\sigma_{\gamma N}$ where $A_{eff}/A \sim .85 \pm .05$. For virtual photons with $Q^2 \geq 1$ GeV^2, $A_{eff}/A \sim 1$. The central question is what variable controls this "shadowing" phenomena. Two very different points of view have been discussed in the literature.

(A) One can argue that fixed Q^2, $\omega = 2m\nu/Q^2 \to \infty$ electroproduction data connects smoothly to $Q^2 = 0$ photoabsorption physics.[21] This "correspondence principle" argument[22] is reinforced by the fact that for large ω, the photon converts to hadronic matter well before the interaction with the nucleus. Thus one predicts that the cross section is shadowed $\left[\nu W_2^A / A\nu W_2^N < 1\right]$ for sufficiently large ω, independent of the value of Q^2. However, there is a momentum sum rule for the area under νW_{2A} (assuming a conventional gluon-quark momentum fraction balance). Thus as noted by Nicolaev and Zakharov,[13] there must be an "anti-shadowing" region probably at $x = \omega^{-1} = m_\pi/m_N$ where $\nu W_2^A > A\nu W_2^N$ [see Fig. 10(a)]. Such a phenomenon would imply to a new type of dynamical interaction between wee partons within the nucleus.

(B) The alternative view,[8] which I favor, is that for $Q^2 > Q_0^2 \sim 1$ GeV^2, $\nu W_2^A(x) = A\nu W_2^N(x)$ for all $x \lesssim 1$. (In addition for $1 \gtrsim x > A$, there is the standard high momentum tail.) [see Fig. 10(b)] Thus for sufficiently large Q^2, the pointlike interactions of virtual photons in the nucleus are essentially incoherent and additive.

More formally, one can write the total photoabsorption cross section in the spectral form[23]

$$\sigma_{\gamma N}(\nu,Q^2) = C\int \frac{d\mathcal{M}^2\,\mathcal{M}^4}{(\mathcal{M}^2+Q^2)^2}\,\sigma_{e^+e^-}(\mathcal{M}^2)\,\sigma_{\mathcal{M}^2}(\nu,Q^2) \qquad (3.1)$$

where $\mathcal{M}$ is the mass of virtual hadronic state which couple to the photon. The spectrum is computed from the e^+e^- annihilation cross section $\sigma_{e^+e^-}(\mathcal{M}^2)$. In order to obtain Bjorken scaling at large ω [modulo logarithmic scale-breaking] the meson-nucleon cross section must behave as $\sigma_{\mathcal{M}^2}(\mathcal{M},Q^2) \sim (\mathcal{M}^2+Q^2)^{-1}$ for large ν. Notice that only $\mathcal{M}^2 \geq O(Q^2)$ contributes to the $\sigma_{\gamma N} \sim (Q^2)^{-1}$ scaling region. But in this region $\sigma_{\mathcal{M}^2}$ is numerically small, and in the case of nuclei, shadowing of the large Q^2 cross section cannot occur![8] The quark-partons of the nucleus at low x thus act independently and incoherently. Further tests of this idea can also be made using the Drell-Yan process $pA \to \mu^+\mu^- X$.

IV. Short-Distance Processes in Nuclei

One of the most interesting questions which can be analyzed using ordinary nuclei is the study of hadronic matter at high density. Here we will be interested in processes such as nuclear form factors at very large momentum transfer, and fast particle production in nuclear collisions (beyond the usual nucleon kinematic limit) each of which probe the high momentum tail of the nuclear wave function. These reactions are sensitive to the behavior of the quark fields in regions of strong overlap.

There is now extensive data (primarily from H. Steiner et al.[24] at LBL) available for the reactions $A_1 + A_2 \to H + X$ for the collisions of

nuclei such as ^{12}C and ^{4}He, at $E_{lab} \lesssim 2$ GeV/nucleon and the production of systems such as $H = \pi$, p, ^{2}H, ^{3}H, ^{4}He at longitudinal momentum k_L well beyond the nucleon-nucleon kinematic limit. In principle the produced hadron H could have nearly all of the momentum of the beam nucleus, but this is clearly exceedingly rare. The question is how rare? Instead of using standard variables such as k_L/k_{Lmax} or E/E_{max}, it is most convenient to use the "light-cone" fraction[25]

$$x = \frac{k_0 + k_3}{P_0 + P_3} \tag{4.1}$$

where k_0 and k_3 are the energy and longitudinal momenta of H and $P_0 + P_3$ are the energy and momentum of A_1. Notice that x is invariant under boosts along P_3. The invariant phase space is $d^3k/k_0 = d^2k_\perp dx/x$ where $\vec{k}_\perp$ is the transverse momentum of H.

The nuclear momentum space wave function [see Fig. 11(a)] can be written as $\Psi_A(x_a, \vec{k}_{\perp a})$, where by momentum conservation $\sum_a \vec{k}_{\perp a} = 0$, $\sum_a x_a = 1$. Since $k_0 = k_3 + (\vec{k}_\perp^2 + m)/(k_0 + k_3)$ for each constituent, the standard energy denominator is

$$\Delta E \equiv P_0 - \sum_a k_0^a$$

$$\Delta E(P_0 + P_3) = M_A^2 - \sum_a \frac{\vec{k}_{\perp a}^2 + m_a^2}{x_a} \tag{4.2}$$

In the adiabatic limit where the binding energy ϵ vanishes, we have $\vec{k}_\perp^2 \to 0$, $x_a \to m_a/M_A$ and $\Delta E \to 0$. Thus $x_a \sim m_a/M_A$ corresponds to the quasi-elastic peak. For example, for the deuteron

$$\Delta E(P_0 + P_3) = M_D^2 - \frac{M_N^2 + \vec{k}_\perp^2}{x} - \frac{M_N^2 + \vec{k}_\perp^2}{1 - x} \qquad (4.3)$$

$$= \begin{cases} M_D^2 - 4M_N^2 - 4\vec{k}_\perp^2 \sim O(M_D\epsilon) & \text{if } x \sim 1/2 \\ M_D^2 - \frac{M_N^2}{0.8} - \frac{M_N^2}{0.2} \sim -2.25\ \text{GeV}^2 & \text{if } x \sim 0.8 \end{cases}$$

Thus, by examining the deuteron wave function in a configuration where one nucleon has 80% of the maximum momentum, the state is probed far off-shell where, in fact, asymptotic freedom perturbative quantum chromodynamic (QCD) calculations should be valid. In this far off-shell regime, the analysis of the high momentum tail of the nuclear wave function clearly involves the synthesis of quark and nuclear physics.

At high energies where cross sections become nearly energy-independent, the reaction $A_1 + A_2 \to H + X$ can be thought of as the materialization of the off-shell wave function[26] [as in Fig. 16]. Thus we expect

$$\frac{dN}{dx}(A_1 + A_2 \to H + X) \equiv \frac{1}{\sigma_{inel}} \int \frac{d^3\sigma}{d^3k/k_0} d^2k_\perp$$

$$= \frac{1}{1-x} \int |\psi(x, \vec{k}_\perp)|^2 \Pi\left[d^2k_{\perp a}\right] \Pi\left[dx_a\right] \qquad (4.4)$$

where the integration is over all unobserved momenta, consistent with momentum conservation. (The inverse factor of 1-x arises from the spectators' phase space.) If we use perturbative QCD then the off-shell kinematics for $x \to 1$ requires the repeated iteration of the QCD scale-invariant kernel in order to "stop" each quark spectator in ψ_{A_1}. Each iteration yields an additional $(1-x)^2$ fall-off, and one readily obtains the "spectator quark counting rule",[26,27,28]

$$\frac{dN}{dx}(H/A) \sim C(1-x)^{2n_s-1} = C(1-x)^{6N_S-1} \qquad (4.5)$$

where n_s is the number of quark spectators (originally bound in A) left behind after forming H. For nuclear problems $n_s = 3N_S$, where N_S is the number of spectator nucleons. The constant C is proportional to the wave function at the origin, i.e., the probability amplitude to find all the quarks at the same point. The spectator counting rule can be derived in QCD, with calculable logarithmic modifications arising from the anomalous dimensions of the hadronic wave function. [In addition one finds that[29] (a) the helicity of A and H tend to match as $x \to 1$, (b) additional spin suppression factors of (1-x) can occur in the case of electromagnetic or weak interaction probes,[29,30] and (c) gluon bremsstrahlung in QCD increase the exponent of (1-x) by a log log s term[31] which is proportional to the color charge[32] (Casimir operator) of H. This latter correction does not occur when H is a hadron.] The simple spectator rule[26] gives $dN/dx \sim (1-x)^3$ for q/p, $(1-x)^1$ for q/M, $(1-x)^5$ for p/D, $(1-x)^9$ for q/D for the leading power of the distribution as $x \to 1$. Notice that the prediction $(1-x)^{65}$ for p/C can also be obtained via the sequential fragmentation $(1-x)^{47}$ for α/C convoluted with $(1-x)^{17}$ for p/α. A comparison of the α/C and p/C predictions with the data of Steiner et al.[24] shown in Fig. 12. A systematic comparison of theory and experiment has been given by Blankenbecler and Schmidt.[28] An effective nucleon-constituent model[28] can also be devised to reproduce (4.5).

The recent forward angle data[24] [see Fig. 13] for p/α apparently indicates two components to the fragmentation distribution, possibily reflecting an intermediate regime from $dN/dx\,(p/d) \sim (0.5-x)^5$. The region beyond $x > 0.4$ is fit to $(1-x)^{15}$ and is not inconsistent with

the $(1-x)^{17}$ prediction. Such comparisons could be more definitive if the light-cone variable x were used.

Although the application of quark-gluon dynamics to such relatively low-energy nuclear data may seen radical, I emphasize that it is justified by the fact that quite far off-shell kinematics are really involved.

Perhaps the most dramatic application of short-distance physics to nuclear targets concerns nuclear form factors at large momentum transfer. The elastic form factor F(t) [with $t = q^2 = -Q^2 < 0$] is the probability amplitude that the target system stays intact and unexcited upon deflection from p to p+q in the electromagnetic collision $eA \to eA$. The dimensional counting rule for the (helicity-conserving) form factor[23]

$$F(t) \sim \frac{1}{t^{n-1}} \qquad \left(|t| >> M^2\right) \tag{4.6}$$

(where n is the minimum number of elementary constituents) reflects the fact that the more complex the target, the faster the power-law fall off. From this formula one predicts $tF_\pi(t)$, $t^2G_M^N(t)$, and $t^5F_D(t)$ are each asymptotically constant. The comparison[34,35] with experiment is shown in Fig. 14. The dimensional counting rule can be rigorously derived in QCD, modulo logarithmic modifications (suppression) from the anomalous dimensions of the hadron wave function; e.g., for the nucleon form factor[36] QCD predicts

$$G_M(t) = \frac{\alpha_s^2(t)}{t^2}\left[\sum_{n=0} a_n \log^{-\gamma_n}(-t/\Lambda^2)\right]^2 \left[1 + \mathcal{O}\left(m^2/t\,,\,\alpha_s(t)\right)\right] \tag{4.7}$$

where the γ_n are known positive numbers (amonalous dimensions) and $\alpha_s(t) \sim C/\log(-t/\Lambda^2)$ is the QCD running coupling constant. In general,

the power law reflects the fact that at large t one must pay a penalty of $\alpha_s(t)/t$ to move a constituent from p to p+q. The usual identification of the form factor with the Fourier transform of the static charge distribution is inapplicable to the relativistic regime.

Is it possible that these quark-gluon results can be applied to systems as complex as nuclei? The answer is certainly yes, although the fact that the momentum transfer must be partitioned among the constituent nucleons implies that the momentum transfer required to reach the truly asymptotic regime increases with A.[35]

Nevertheless, the quark concept is useful in the subasymptotic domain where the nucleus can still be regarded as a bound state of nucleons. For example, the deuteron form factor $F_D(t)$ must clearly fall at least as fast as $F_p(t/4)\cdot F_n(t/4)$ since each nucleon must change momentum from $\sim p/2$ to $\sim(p+q)/2$ and stay intact. Thus we should consider the "reduced" form factor $f_D(t)$ defined via[35,37]

$$F_D(t) \equiv F_p(t/4)\, F_n(t/4)\, f_D(t) \tag{4.8}$$

Note that $f_D(t)$ must decrease at large t since it can be identified the probability amplitude for the final state n-p system to remain a ground state deuteron. In fact, the dimensional counting formula (4.6) implies[35,37]

$$f_D(t) \sim \frac{1}{t} \tag{4.9}$$

In general, we can define the reduced nuclear form factor

$$f_A(t) \equiv \frac{F_A(t)}{\prod_{i=1}^{A} F_N(t/A^2)} \tag{4.10}$$

which has the effect of the nucleon form factors removed. By dimensional counting $f_A(t) \sim 1/t^{A-1}$ (as if the nucleons were elementary!), and one expects this result to hold even for moderate values of $|t|$. In contrast, the complete scaling of $F_A(t) \sim t^{1-3A}$ requires very large momentum transfer.[35]

A comparison of the data for $f_D(t)$ with the prediction $t\, f_D(t) \to$ const. is shown in Fig. 15. The asymptotic regime seems to hold for $|t| \geq 1$ GeV^2. Recent data[38] on inelastic electron scattering on deuterons also indicate that the inelastic transfer form factors $\gamma + D \to X$ where m_X^2 is below the pion threshold have a similar behavior. Although, the comparisons with experiment are less decisive, the ^{3}He and ^{4}He high momentum transfer form factors measured at SLAC by Chertok et al.[39] also appear to be consistent with the scaling behavior predicted by Eq. (4.10) [see Fig. 16].

The types of diagram one encounters when computing the deuteron form factor are shown in Fig. 17. Diagram (a) corresponds to a simple "democratic" chain model.[35] Because a single gluon cannot couple to a color singlet, this contribution only is relevant for the part of the nuclear state which contains "mixed color", i.e., does not correspond to a state which can be separated into two color singlet 3 quark systems. The asymptotic form factor for such diagrams behaves as $F_n(t) \sim C/(|t| + m_n^2)^{n-1}$ where $m_n^2 \sim n m_1^2$ and $n = 3A$ for nuclei. For the deuteron state with an ordinary two-nucleon color singlet wave function, the quark interchange diagram of Fig. 17(b) contributes, and gives a contribution of the form of Eq. (4.8) with $f_D(t) \sim C/(|t| + m_0^2)$. This contribution can also be identified with the standard amplitude of Fig. 17(c) where

$T_{np \to np} \propto 1/t^4$ is the off-shell np scattering amplitude at $\theta_{cm} = 90^o$. Exchange current (meson-exchange) contributions can also be identified with this amplitude.

In general, one expects that the deuteron ground state consists of a linear combination of a standard color singlet $|np\rangle$ wave function plus a "mixed color" $|6q\rangle$ amplitude. The latter component has a high energy (~270 MeV) in the MIT Bag Model, but it in fact may dominate the high momentum components of the wave function since the np state is suppressed by short range repulsion of the n-p interaction at small distances.[40] Dubokov and Kobushkin[41] have argued that the $|6q\rangle$ mixed color component can account for the anomalous photon polarization seen in $np \to d\gamma$. The $|6q\rangle$ mixed color state is the prototype of new quark matter which, if QCD is correct, must exist within the nuclear wave function. It clearly deserves much more study.

V. Conclusion

As I have outlined in this talk, there now is substantial evidence that the quark and gluon degrees of freedom play a role in phenomena involving ordinary nuclear matter. This evidence is based on the successful predictions based on QCD from

(a) Elastic form factors of nuclei at large momentum transfer,

(b) the tail of the momentum distribution in nuclei observed in fast particle production in nuclear collisions, and, possibly,

(c) the multiplicity distribution observed in nucleon-nucleus and lepton-nucleus scattering.

It is important to explore these phenomena more thoroughly, both by use of higher energy and higher momentum transfer experiments, as well as more theoretical analysis. I should emphasize that the processes (a) and (b) probe amplitudes where quarks are in close proximity, and mixed color states may be playing an important role.

Studies of the final state in deep inelastic processes, especially the Drell-Yan reaction $A+B \to \ell\bar{\ell}X$, inelastic lepton scattering $\ell A \to \ell' X$, and the production of hadrons and jets at large transverse momentum are especially interesting since in such reactions one can study the evolution of colored matter through the nuclear medium.[42] The energy loss patterns of leading particles are particularly interesting.[43] It is also important to determine what are the essential parameters (Q^2 or ω?) which control shadowing of the structure functions and photoabsorption cross section.

Elastic scattering large momentum transfer experiments on nuclei, although difficult, are also of considerable interest. For example, large angle $K^{\pm}$-nucleus scattering can test whether quark interchange mechanisms are dominant.[44] The momentum transfer dependence of such reactions can be predicted using the reduced form factor analysis of Section IV and Ref. 27.

The analysis of nucleus-nucleus collisions which I have presented here is conventional in the sense that I have used only standard features of quark and gluon physics. On the other hand, there could be further surprises as one approaches a new regime of high-energy heavy ion collisions where nuclear matter is forced into new configurations. In any event, we are clearly only at the beginning of the study of high energy processes within the nuclear environment.

ACKNOWLEDGEMENTS

I would like to thank A. Białas, R. Blankenbecler, T. Burnett, B. Chertok, J. Gunion, G. P. Lepage, M. Kühn and I. Schmidt for helpful conversations. The color-neutralization model discussed here is based on an earlier parton model developed in collaboration with J. Gunion and H. Kühn. I would also like to thank M. Gyulassy for invited me to this workshop.

REFERENCES

1. For a comprehensive review of possible anomalous nuclear phenomena see W. Greiner, report to this conference.
2. Current ideas on the application of quark and gluon physics to nuclear reactions are discussed in A. Białas, FERMILAB-Conf. 79/35 (this conference); N. N. Nikolaev, A. Ya. Ostapchuck and V. R. Zoller, CERN preprint TH-2541; N. N. Nicolaev and S. Pokorski, Phys. Lett. 80B, 290 (1979); and Z. J. Rek and G. Wilk, Phys. Lett. 78B, 333 (1978).
3. R. P. Feynman, "Photon-Hadron Interactions," W. A. Benjamin, Inc., 1972, and unpublished.
4. For recent data and reviews see Ref. 2; T. Ferbel, this conference, W. Busza, Acta. Phys. Pol. B8, 333 (1977); D. Cutts et al., Fermilab-Pub-79/44 (1979); J. E. Elias et al., Fermilab-Pub-79/47 (1979); C. Halliwell, Proc. of the VIII International Symposium on Multiparticle Dynamics, Kaysersberg, France (1977); and W. Busza, Proc. of the VII International Colloquium on Multiparticle Reactions, Tutzing, Germany (1976).
5. F. Low, Phys. Rev. D12, 163 (1975).
6. S. Nussinov, Phys. Rev. Lett. 34, 1286 (1973).
7. S. J. Brodsky and J. F. Gunion, Phys. Rev. Lett. 37, 402 (1976), and Proc. of the VII International Colloquium on Multiparticle Reactions, Tutzing, Germany (1976).
8. S. J. Brodsky, J. F. Gunion and J. Kühn, Phys. Rev. Lett. 39, 1120 (1977).
9. For discussions and references, see A. Białas, Ref. 2.

10. W. Busza, Ref. 4.

11. S. A. Azimov et al., Phys. Lett. B73, 500 (1978). See also N. N. Nikolaev et al., Ref. 2.

12. A. Capella and A. Krzywicki, Phys. Rev. D18, 3357 (1978), Phys. Lett. 67B, 84 (1977).

13. V. I. Zakharov, N. N. Nikolaev, Sov. J. Nucl. Phys. 21, 227 (1975); V. I. Zakharov, Proc. of the 18th International Conference on High Energy Physics, Tbilisi (1976).

14. A. Bałas, Fermilab-Conf-79/35-THY (this conference); A. Bialas, W. Czyż and W. Furmanski, Acta. Phys. Pol. 88, 585 (1977); A. Bałas, Fermilab-Pub-78/75-THY (1978); see also A. Bałas and E. Bałas, Fermilab-Pub-79/48-THY (1979); A. Bałas, M. Blesyznski and W. Czyż, Nucl. Phys. B111, 461 (1976).

15. M. F. Kaplan and D. M. Ritson, Phys. Rev. 85, 932 (1952).

16. Note that this differs from the prediction of the parton model of Ref. 8.

17. L. Hand et al., Acta. Phys. Pol. B9, 1987 (1978), Cracow preprint INP-1019/PH (1978). See also H. C. Ballagh et al., Phys. Lett. 79B, 320 (1978), and references therein.

18. L. Mandansky, private communication.

19. W. R. Ditzler et al., Phys. Lett. 57B, 201 (1975).

20. J. Eickmeyer et al., Phys. Rev. Lett. 36, 289 (1976); R. Talman, Phys. Rev. D15, 1260 (1977). A complete review of nuclear shadowing is given in T. H. Bauer, R. D. Spital, D. R. Yennie and F. M. Pipkin, Rev. Mod. Phys. 50, 261 (1978); and G. Grammer and J. D. Sullivan, Illinois preprint ILL-TH-77-20 (1977), published in "Electromagnetic Interactions of Hadrons," eds. by A. Donnachie, G. Shaw, Plenum Press.

21. J. D. Bjorken, Acta. Phys. Pol. B2, 5 (1975), and lectures at the DESY Summer Institute (1975). H. Harari, Proc. of the 1971 International Symposium on Electron and Photon Interactions at High Energies, Cornell.

22. J. D. Bjorken and J. B. Kogut, Phys. Rev. D8, 1341 (1973).

23. S. J. Brodsky and J. Pumplin, Phys. Rev. 182, 1794 (1969); V. Gribov, Zh. Eksp. Teor. Fiz. 57, 1306 (1969) [Sov. Phys. JETP 30, 709 (1970)]; S. Brodsky, G. Grammer, G. P. Lepage and J. Sullivan (unpublished).

24. M. C. Lemaire et al., LBL-8463 (1978); H. Steiner, LBL-6756, published in Proc. of the VII International Conference on High Energy Physics and Nuclear Structure, Zurich (1977).

25. See, e.g., S. Weinberg, Phys. Rev. 150, 1313 (1966); L. Susskind and G. Frye, Phys. Rev. 165, 1535 (1968); S. J. Brodsky, R. Roskies and R. Suaya, Phys. Rev. D8, 4574 (1973); M. G. Schmidt, Phys. Rev. D9, 408 (1974); R. Blankenbecler and S. J. Brodsky, Phys. Rev. D10, 2973 (1974) and references therein.

26. R. Blankenbecler and S. J. Brodsky, Ref. 25; J. F. Gunion, UC-Davis preprint UCD-79-4 (1979), and references therein.

27. S. J. Brodsky and B. T. Chertok, Phys. Rev. Lett. 37, 269 (1976); Phys. Rev. D14, 3003 (1976).

28. R. Blankenbecler and I. Schmidt, SLAC-PUB-2010, Proc. of the 8th International Symposium on Multiparticle Dynamics, Kaysersberg, France (1977); Phys. Rev. D15, 3321 (1977).

29. G. R. Farrar and D. R. Jackson, Phys. Rev. Lett. 35, 1416 (1975); S. J. Brodsky and G. P. Lepage, SLAC-PUB-2294 (1979).

30. E. L. Berger and S. J. Brodsky, Phys. Rev. Lett. 42, 940 (1979).

31. See, e.g., Yu. L. Dokshitser, D. I. Dyakanov and S. I. Troyan, SLAC-TRANS-0183 (1978), translated from Proc. of the 13th Leningrad Winter School of Elementary Particle Physics (1978).

32. S. J. Brodsky and G. P. Lepage, Ref. 29.

33. S. J. Brodsky and G. R. Farrar, Phys. Rev. Lett. 31, 1153 (1973) and Phys. Rev. D11, 1309 (1975); V. A. Matveev, R. M. Muradyan and A. V. Tavkheldzie, Lett. Nuovo Cimento 7, 719 (1973).

34. R. G. Arnold, SLAC-PUBS-2334 and 2373 (1979).

35. S. J. Brodsky and B. T. Chertok, Ref. 27.

36. G. P. Lepage and S. J. Brodsky, SLAC-PUB-2348 (1979), to be published in Phys. Rev. Lett.

37. S. J. Brodsky, SLAC-PUB-1497, published in the Proc. of the International Conference on Few Body Problems in Nuclear and Particle Physics, Quebec (1974).

38. F. Martin et al., Phys. Rev. Lett. 38, 1320 (1977); W. P. Schutz et al., Phys. Rev. Lett. 38, 259 (1977).

39. R. G. Arnold et al., Phys. Rev. Lett. 40, 1429 (1978); B. T. Chertok, Phys. Lett. 41, 1155 (1978).

40. V. A. Matveev and P. Sorba, Nuovo Cimento Lett. 20, 435 (1977). See also A. P. Kobushkin, Kiev preprint ITF-77-113E (1977).

41. V. M. Dubovik and A. P. Kobushkin, Kiev preprint ITF-78-85E (1978).

42. A model of particle production at large transverse momentum which takes into account gluon interactions is given by A. Krzywicki, J. Engles, B. Petersson and U. Sukhatme (1979).

43. A. Dar and F. Tagaki, Technion preprint PH-79-28 (1979).

44. S. J. Brodsky and J. Kühn (unpublished).

FIGURE CAPTIONS

1. (a) Simplified representation of particle production in a simple color-gluon exchange model.

   (b) Rapidity distribution of particles produced in a simplified model where hadron production is proportional to the soft gluon distribution [see Ref. 7].

2. Schematic representation of hadron-nucleus interactions in a color excitation/neutralization model. An event where 3 nucleons are "wounded" is shown.

3. (a) Schematic representation of the rapidity distribution of hadrons produced in hadron-nucleus collisions for the "event" of Fig. 2. The distribution is normalized to hadron-nucleon collisions.

   (b) Rapidity distribution ratio obtained after averaging over events of the type of Fig. 2, assuming interactions occur uniformly in rapidity in the nucleus.

4. (a) Comparison of the prediction of Eq. (2.4) with the data of Ref. 10 for the A-dependence of particle production in nuclei.

   (b) Comparison of the prediction of Eq. (2.1) with data for particle production in proton-emulsion collisions (normalized to pp-collisions). The value $\bar{\nu} = 3$ is used. The predictions for the fragmentation regions must be modified to take into account nuclear fragment cascading for $y < y_A$ and energy-momentum losses of fast particle for $y > y_H$. The data are from Ref. 11.

5. Idealized predictions of various models for the rapidity distribution of hadron production in nucleus-nucleus $A + B \rightarrow X$ collisions, normalized to nucleon-nucleon collisions (see text).

6. Theoretical predictions for particle production in nucleus-nucleus collisions $A+B \to X$ normalized to nucleon-nucleon collisions. The color-neutralization model discussed in Section II (and also in Ref. 8) is compared with the quark-constituent model of Bialas et al., Ref. 14.
7. Schematic representation of sequential gluon exchange for meson collisions. The statistical average over events gives the same result as an incoherent sum of single-gluon exchange events.
8. Schematic representation of particle production in nuclei for deep inelastic lepton scattering.
9. (a) Comparison of particle production for μ^+ emulsion inelastic scattering at $p_{lab} = 150$ GeV/c with hadron-emulsion data (with incident hadron momenta chosen to roughly match the effective virtual photon energy).

   (b) The ratio of muon-nucleus to muon-nucleon multiparticles as a function of $\omega = -q\cdot p_N/q^2$. The data are from Ref. 17.
10. Schematic representation of the ratio of the deep inelastic lepton scattering structure functions $\nu W_2^A/A\nu W_2^N$ illustrating (a) the possibility of shadowing and anti-shadowing region, or (b) the possibility that there is no shadowing for sufficiently large Q^2. Here $x = -q^2/2q\cdot p_N$, $0 < x < A$.
11. (a) Illustration of the momentum-space wave function for a nuclear bound state using the light-cone/infinite momentum frame variables.

    (b) Mechanism for the production of hadrons or sets of quarks or gluons via Pomeron or gluon exchange.

12. Comparison of the spectator counting rule Eq. (4.5) with α and p production in ^{12}C-C collisions at p_{lab} = 1.05 GeV/nucleon. The data for the inclusive cross sections are from Ref. 24. A systematic comparison of theory and experiment is given in Ref. 28.

13. Inclusive cross section for $\alpha + C \to p + X$, compared with the p/α and p/d predictions of the spectator counting rule. The data are from Ref. 24.

14. Comparison of the dimensional counting rule $t^{n-1}F(t) \to$ const. ($|t| >> M^2$) with data. The compilation is from Ref. 34 and references therein.

15. The reduced form factor of the deuteron, divided by a monopole form factor. Dimensional counting predicts this ratio should approach a constant at large t. The data are from Ref. 38.

16. Form factor data from Ref. 39 for ^{2}H, ^{3}He and ^{4}He compared to the quark interchange model predictions of Ref. 35.

17. (a) Example of a simple gluon exchange mechanism for the deuteron form factor at large t.
    (b) Quark-interchange contribution to the deuteron form factor.
    (c) Relationship of the deuteron form factor to off-shell n-p scattering.

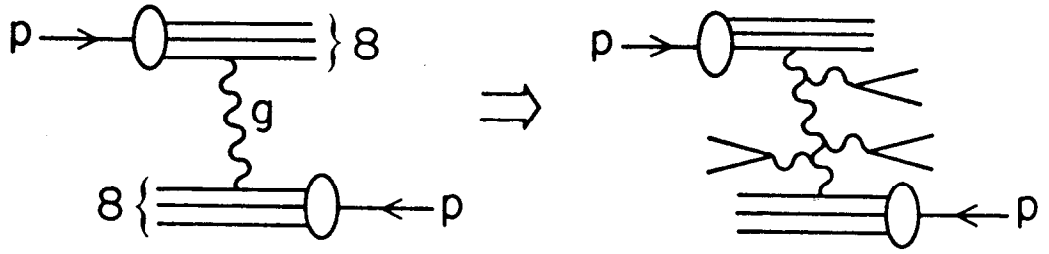

(a)

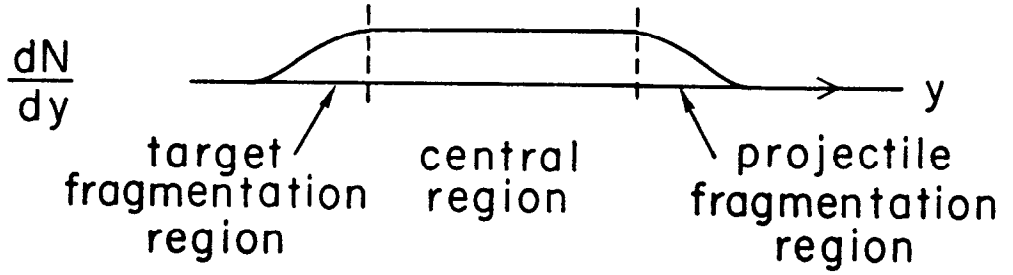

(b)

8-79

3675A1

Fig. 1

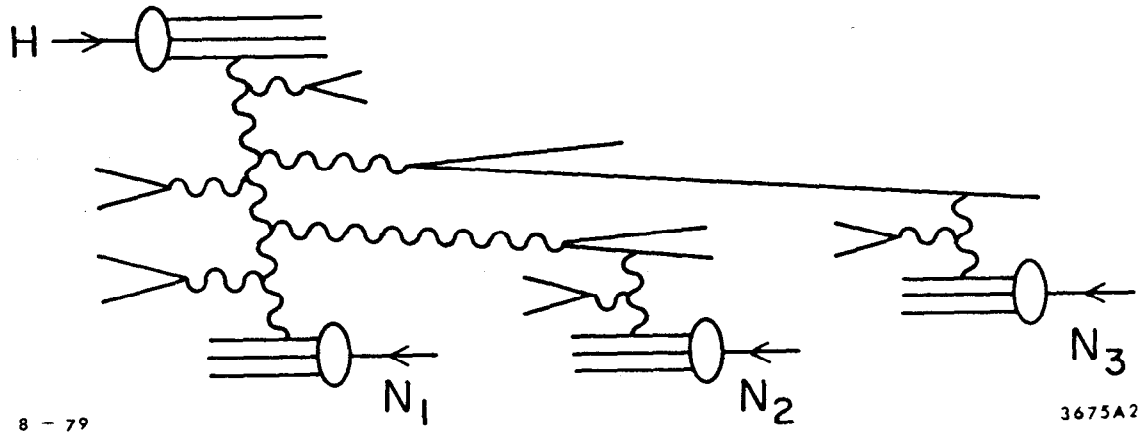

Fig. 2

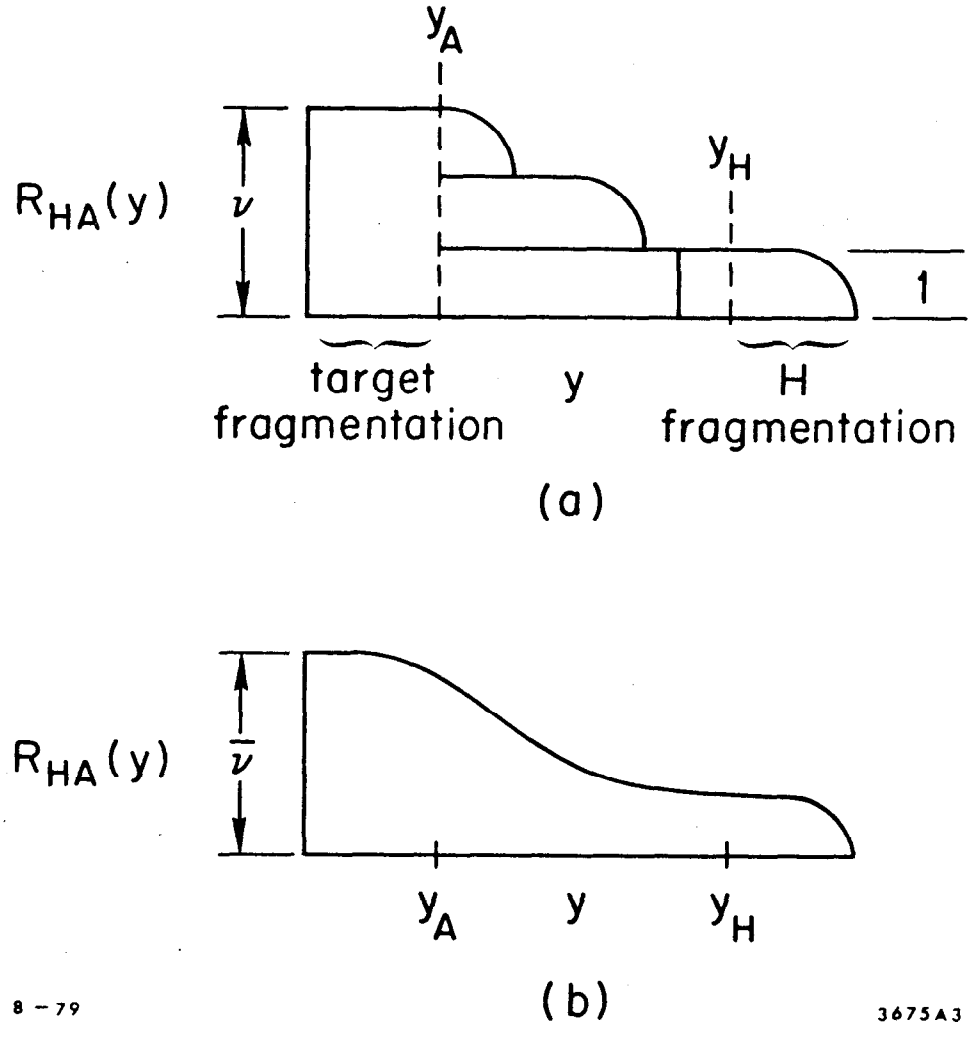
y_A
y_H
$R_{HA}(y)$
ν
1
target fragmentation
y
H fragmentation
(a)
$R_{HA}(y)$
$\bar{\nu}$
y_A
y
y_H
(b)
8 – 79
3675A3

Fig. 3

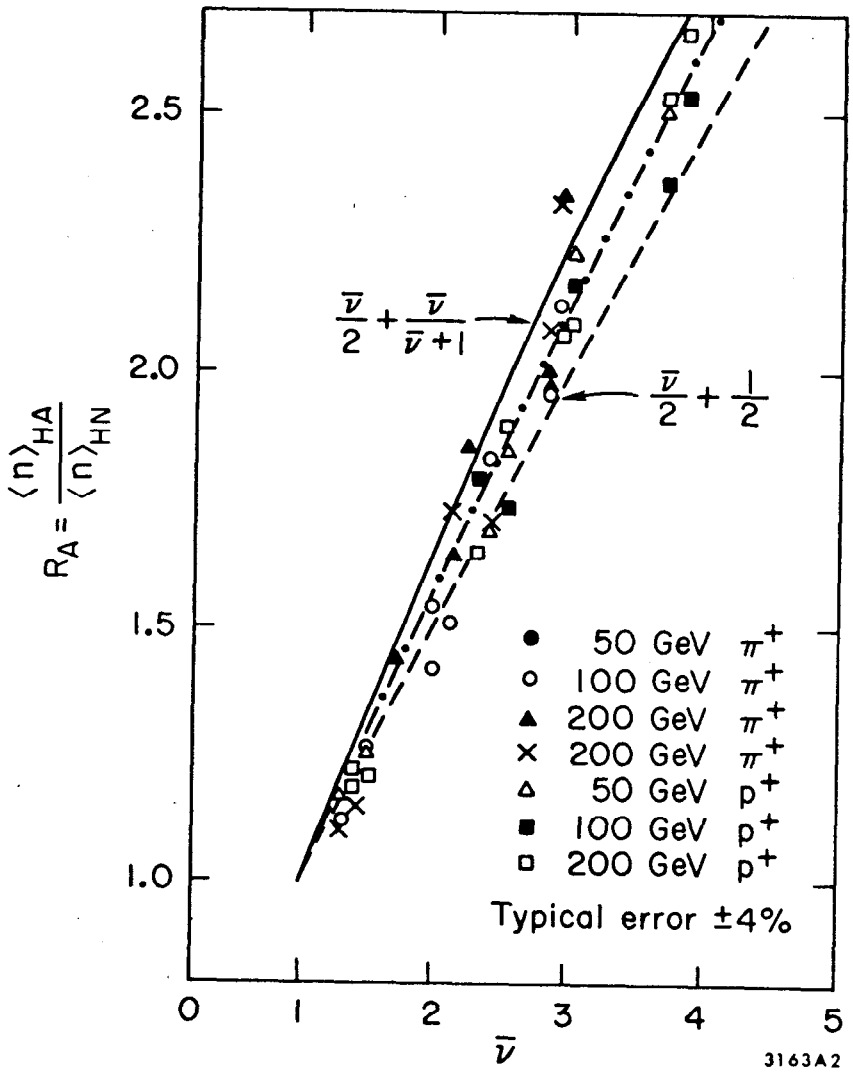
$R_A = \frac{\langle n \rangle_{HA}}{\langle n \rangle_{HN}}$
2.5
2.0
1.5
1.0
0
1
2
3
4
5
$\bar{\nu}$
$\frac{\bar{\nu}}{2} + \frac{\bar{\nu}}{\bar{\nu}+1}$
$\frac{\bar{\nu}}{2} + \frac{1}{2}$
50 GeV π^+
100 GeV π^+
200 GeV π^+
200 GeV π^+
50 GeV p^+
100 GeV p^+
200 GeV p^+
Typical error ±4%
3163A2

Fig. 4a

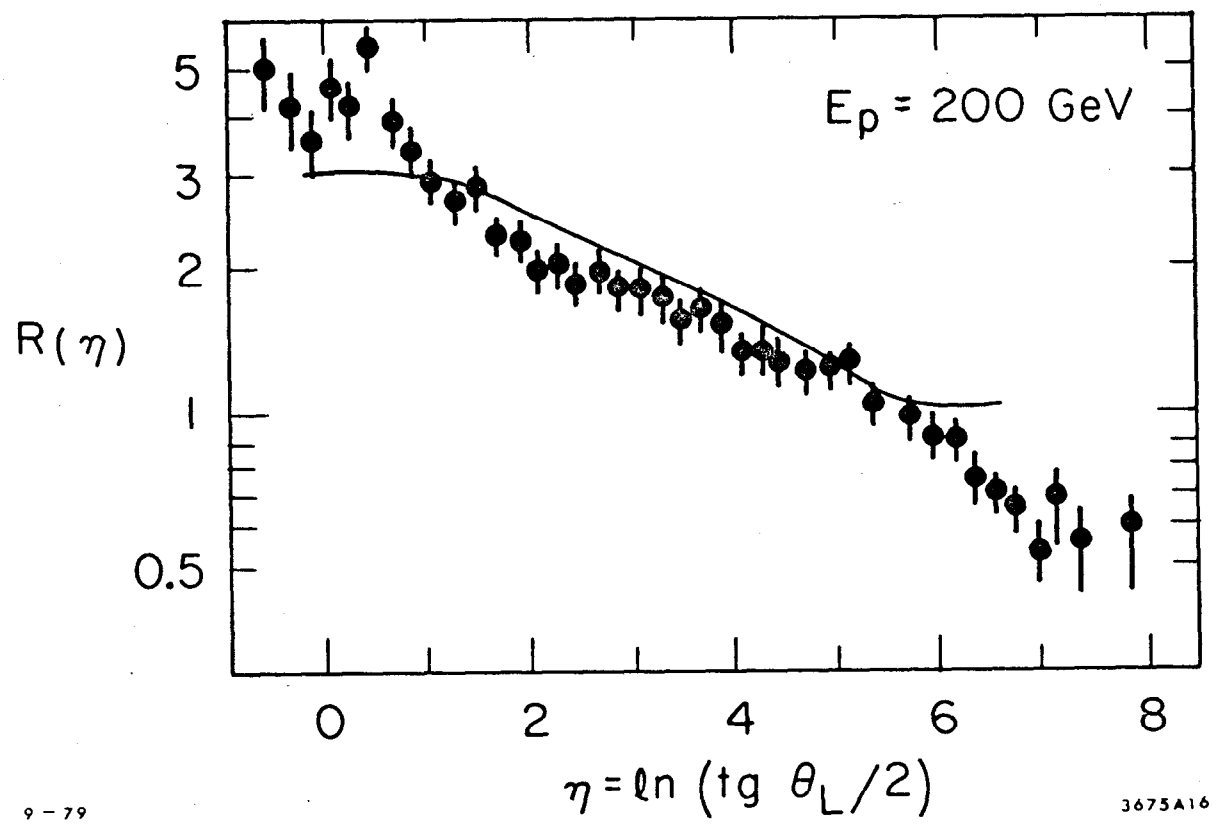

Fig. 4b

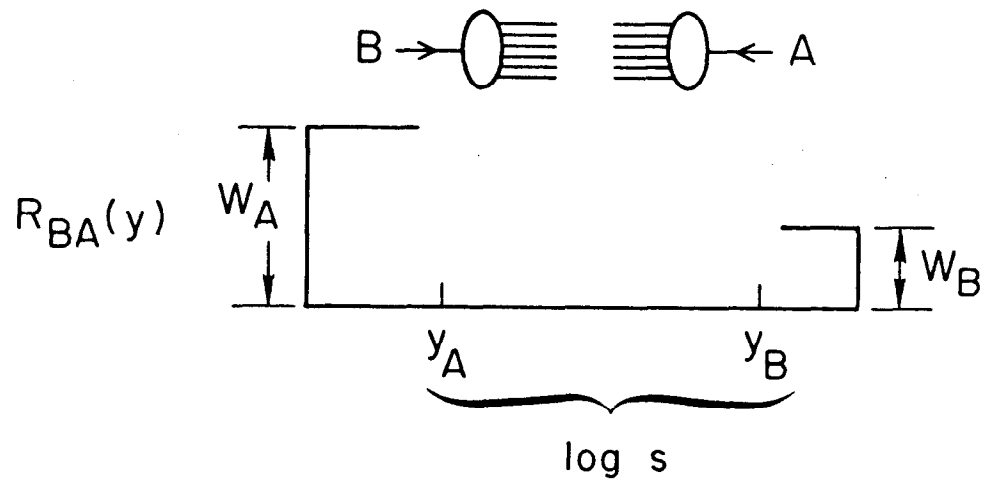

(a)

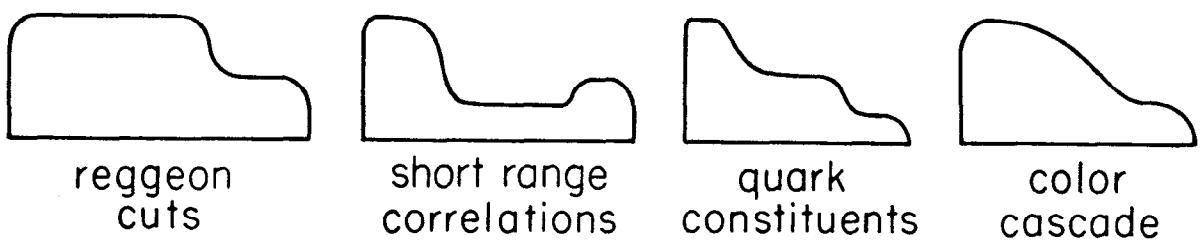

(b)

9 – 79

3675A4

Fig. 5

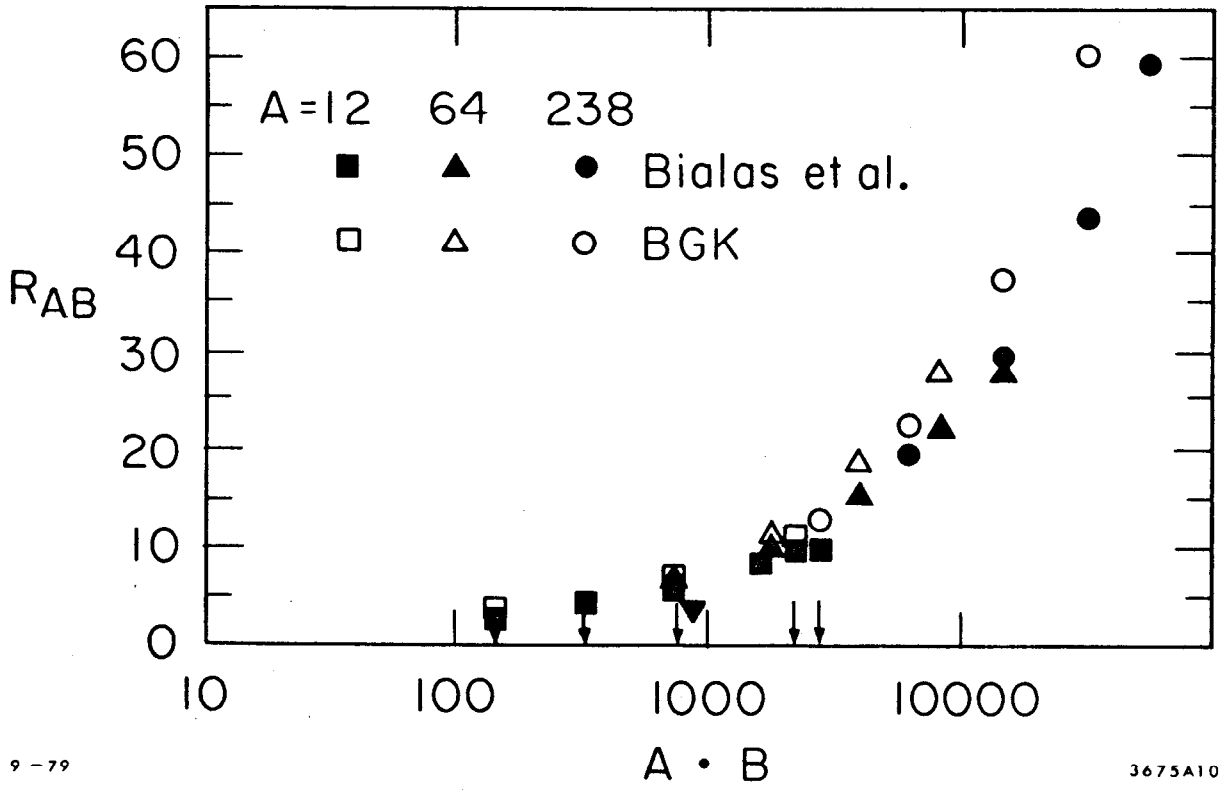
60
50
40
30
20
10
0
A=12 64 238
Bialas et al.
BGK
R_{AB}
10
100
1000
10000
A • B
9-79
3675A10

Fig. 6

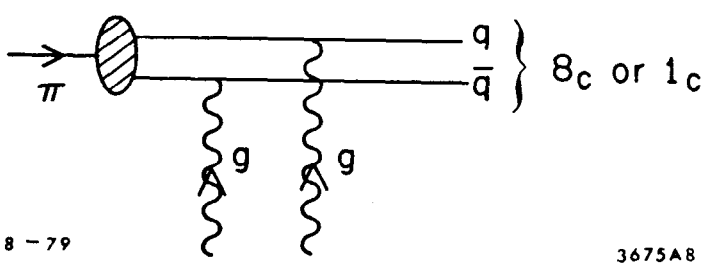

Fig. 7

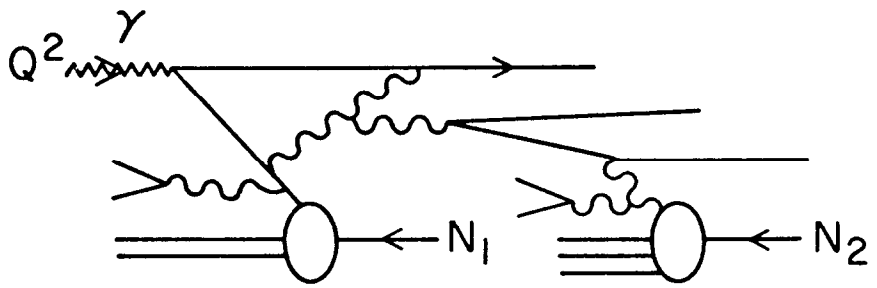

9 – 79 3675A9

Fig. 8

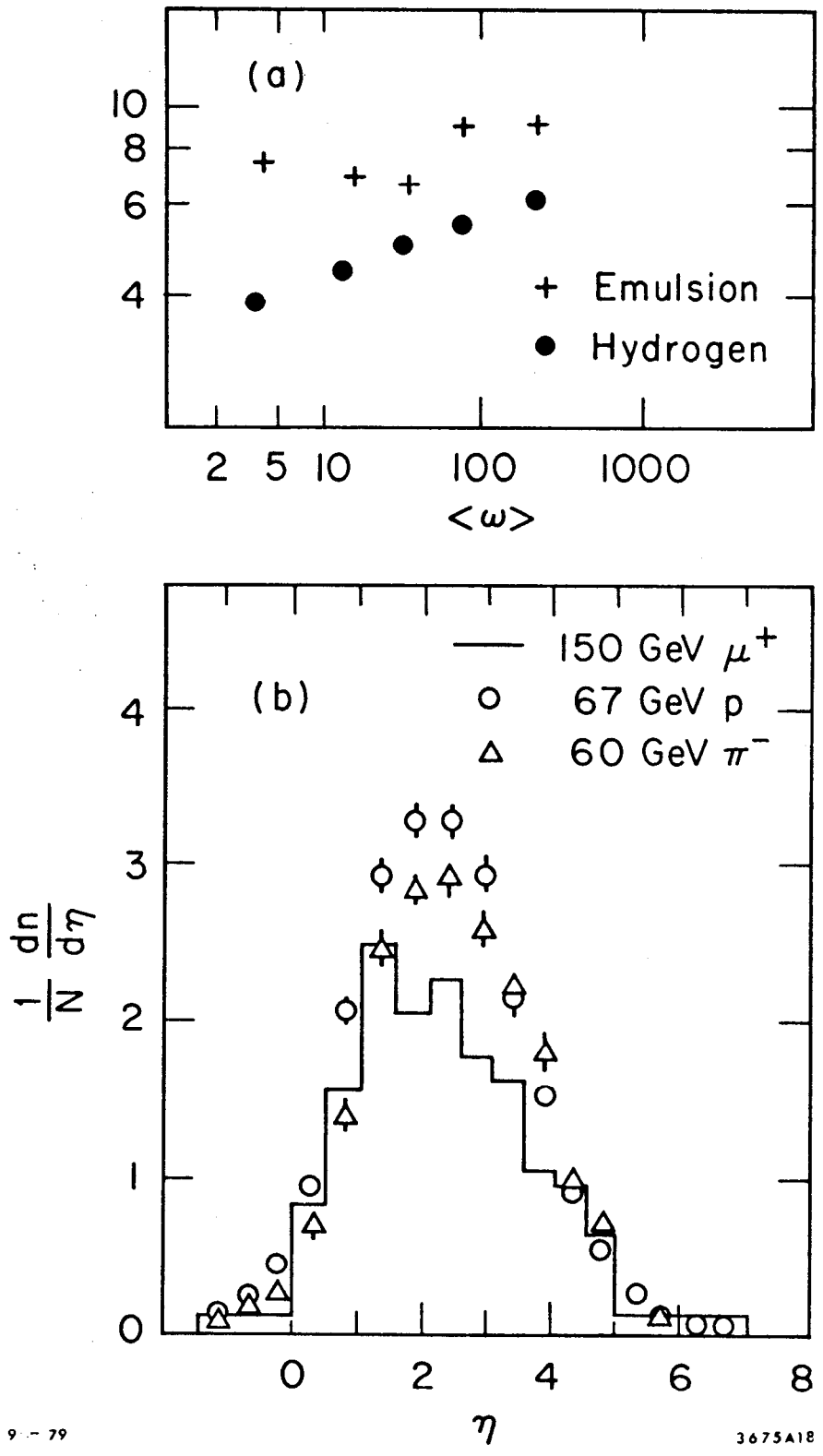
(a)
10
8
6
4
+ Emulsion
● Hydrogen
2 5 10 100 1000
<ω>
(b)
150 GeV μ+
67 GeV p
60 GeV π−
4
3
2
1
0
1/N dn/dη
0 2 4 6 8
η
9 - 79
3675A18

Fig. 9

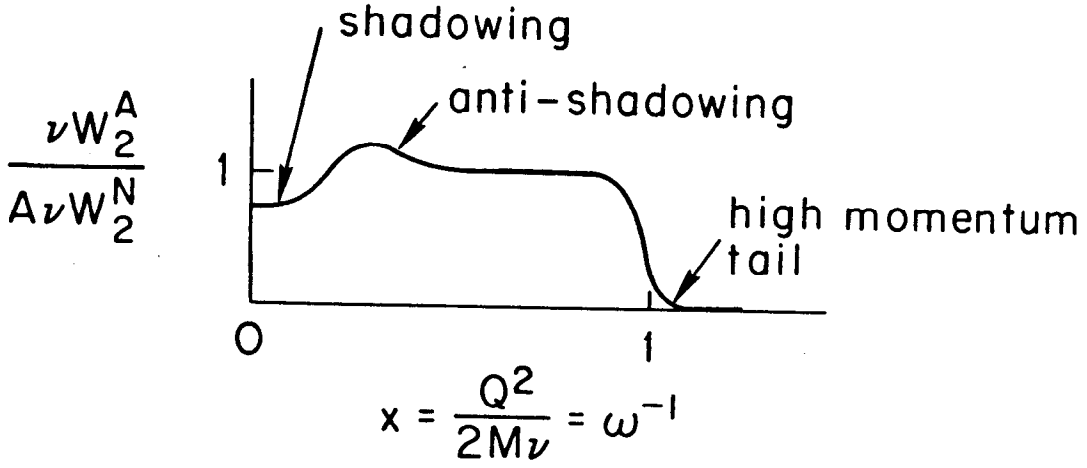

(a)

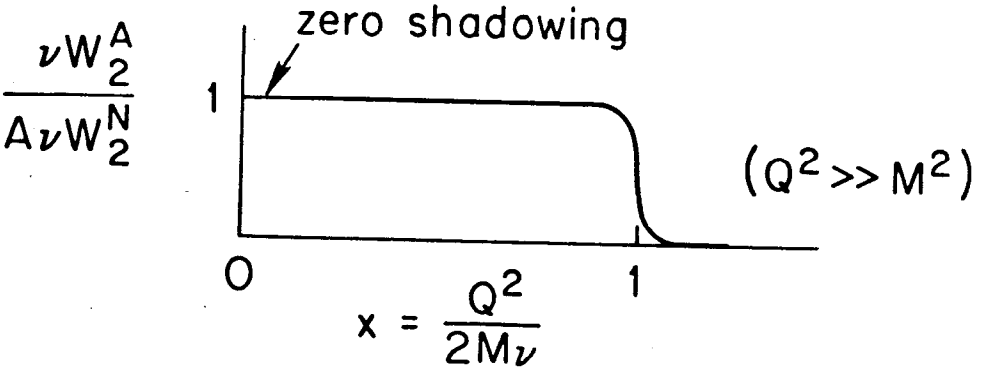

(b)

8-79

3675A7

Fig. 10

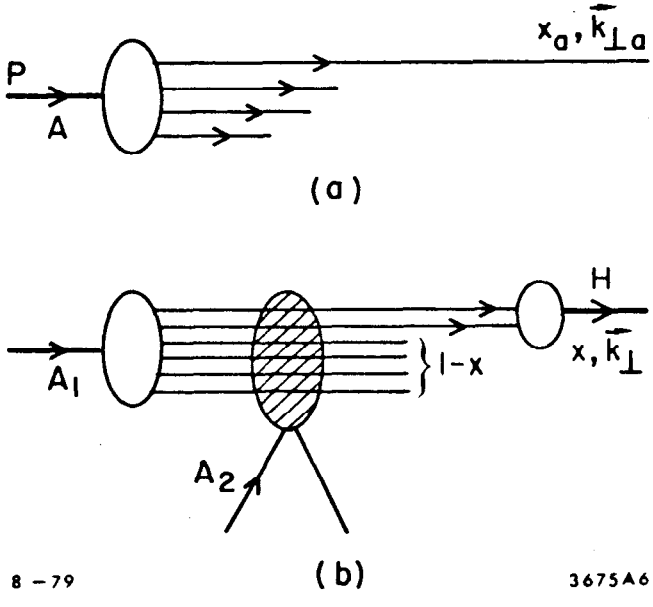

Fig. 11

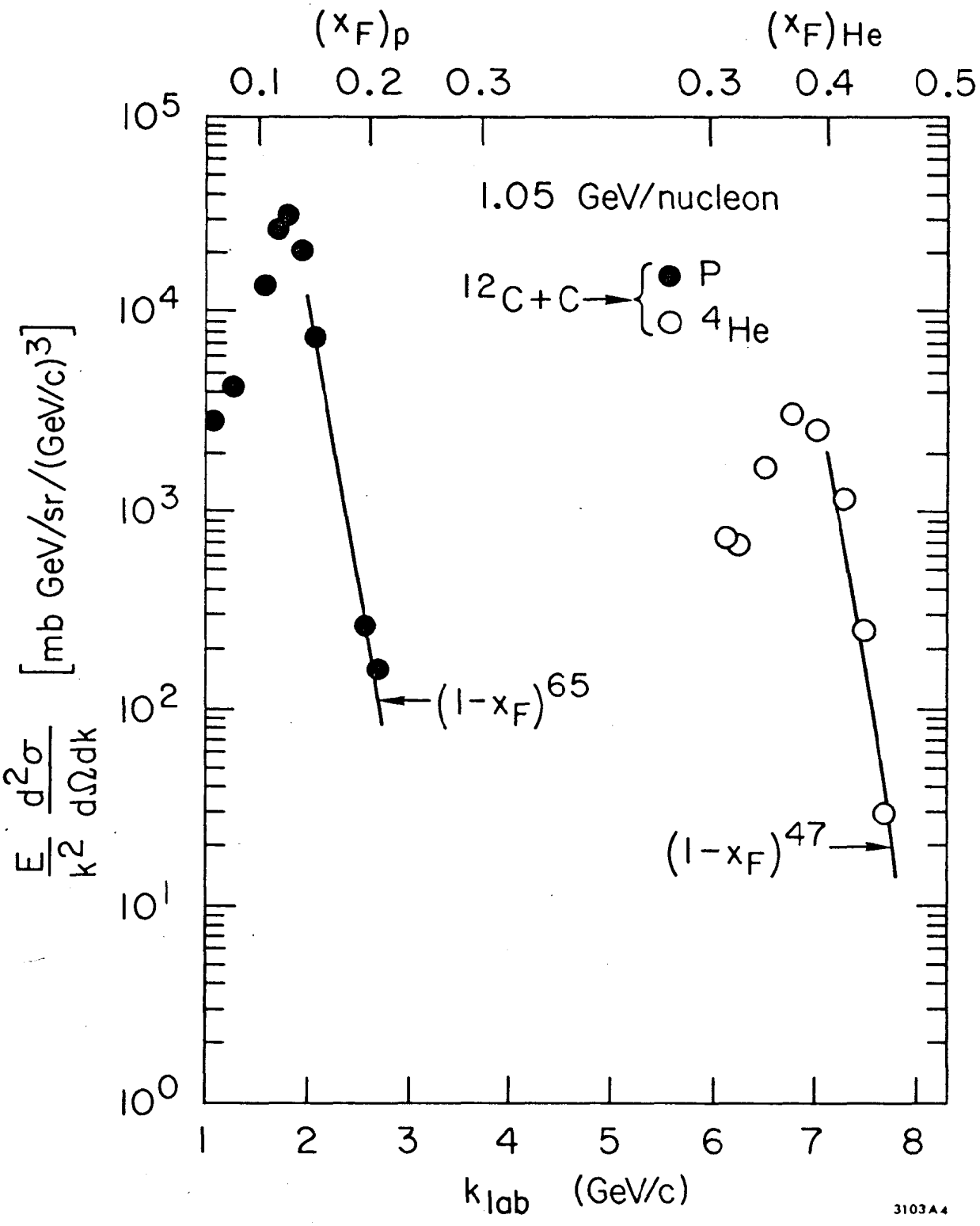
$(x_F)_p$
$(x_F)_{He}$
0.1
0.2
0.3
0.3
0.4
0.5
10^5
10^4
10^3
10^2
10^1
10^0
1.05 GeV/nucleon
$^{12}C+C \rightarrow$ P
^4He
$(1-x_F)^{65}$
$(1-x_F)^{47}$
$\frac{E}{k^2}\frac{d^2\sigma}{d\Omega dk}$ [mb GeV/sr/(GeV/c)^3]
1
2
3
4
5
6
7
8
k_{lab} (GeV/c)
3103A4

Fig. 12

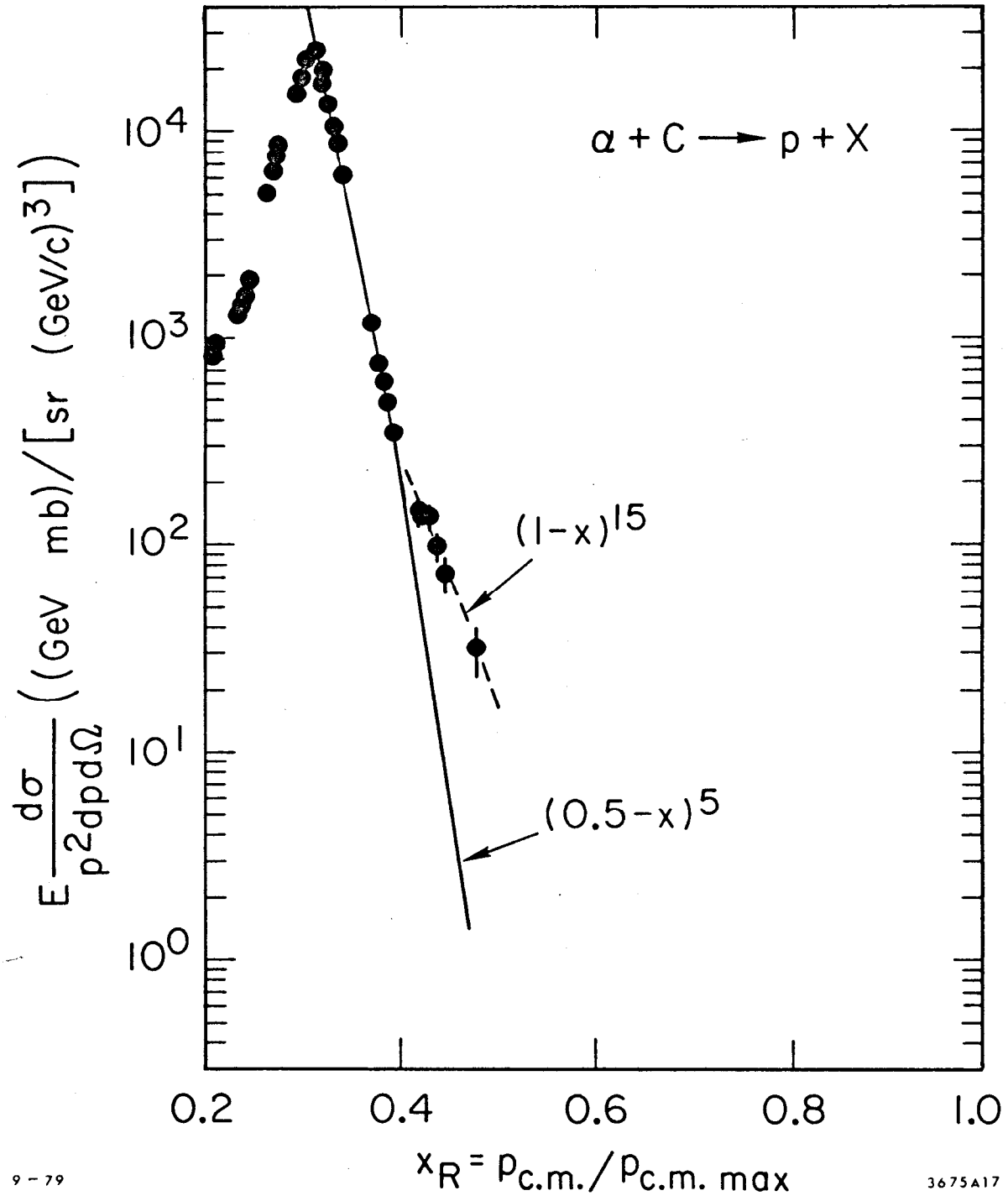
$\alpha + C \longrightarrow p + X$
$E\frac{d\sigma}{p^2 dp d\Omega}$ ((GeV mb)/[sr (GeV/c)^3])
10^4
10^3
10^2
10^1
10^0
$(1-x)^{15}$
$(0.5-x)^5$
0.2
0.4
0.6
0.8
1.0
$x_R = p_{c.m.}/p_{c.m.\ max}$
9-79
3675A17

Fig. 13

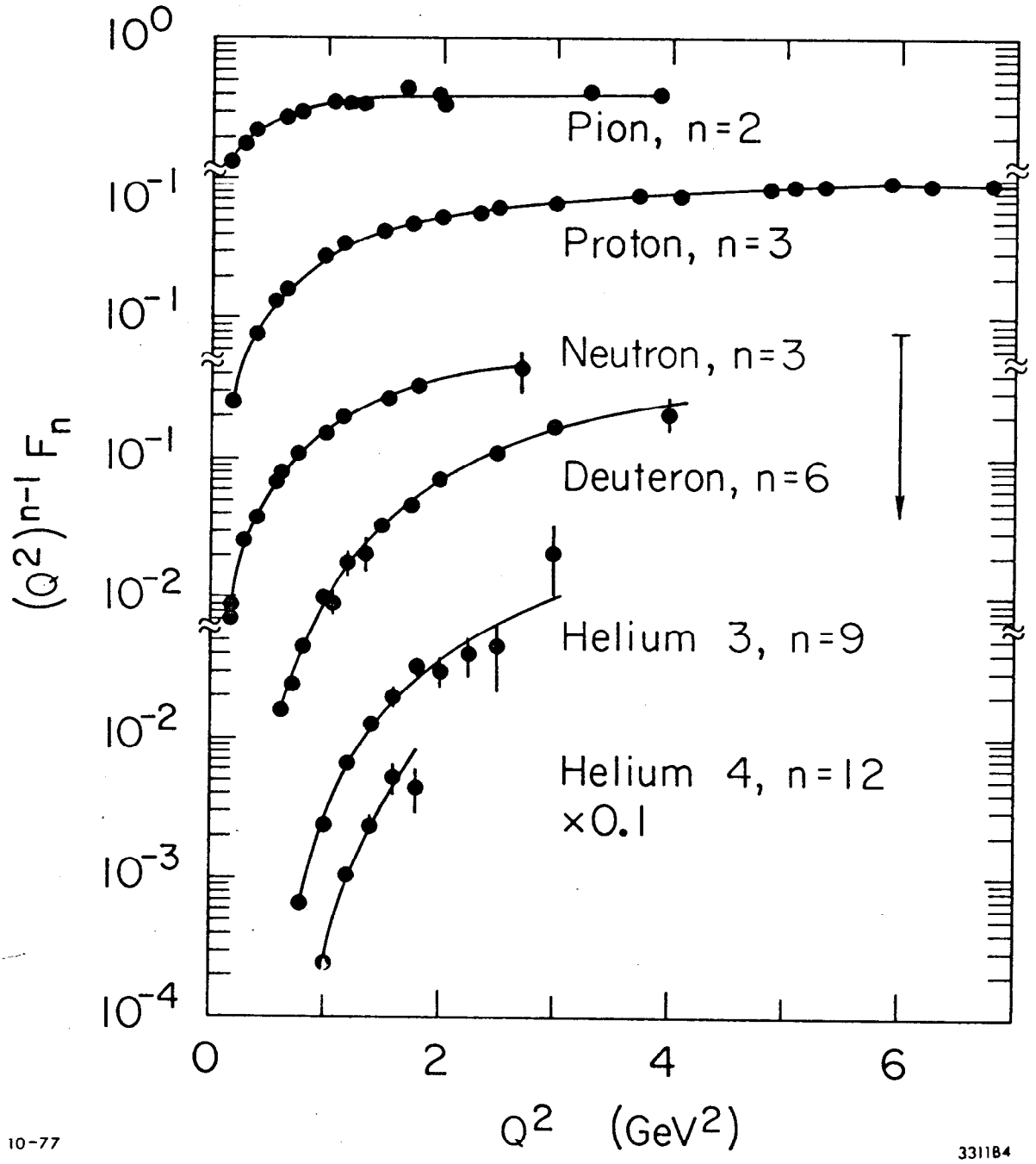
10^0
10^{-1}
10^{-1}
10^{-1}
10^{-2}
10^{-2}
10^{-3}
10^{-4}
$(Q^2)^{n-1} F_n$
Pion, n=2
Proton, n=3
Neutron, n=3
Deuteron, n=6
Helium 3, n=9
Helium 4, n=12
×0.1
0
2
4
6
Q^2 (GeV^2)
10-77
331184

Fig. 14

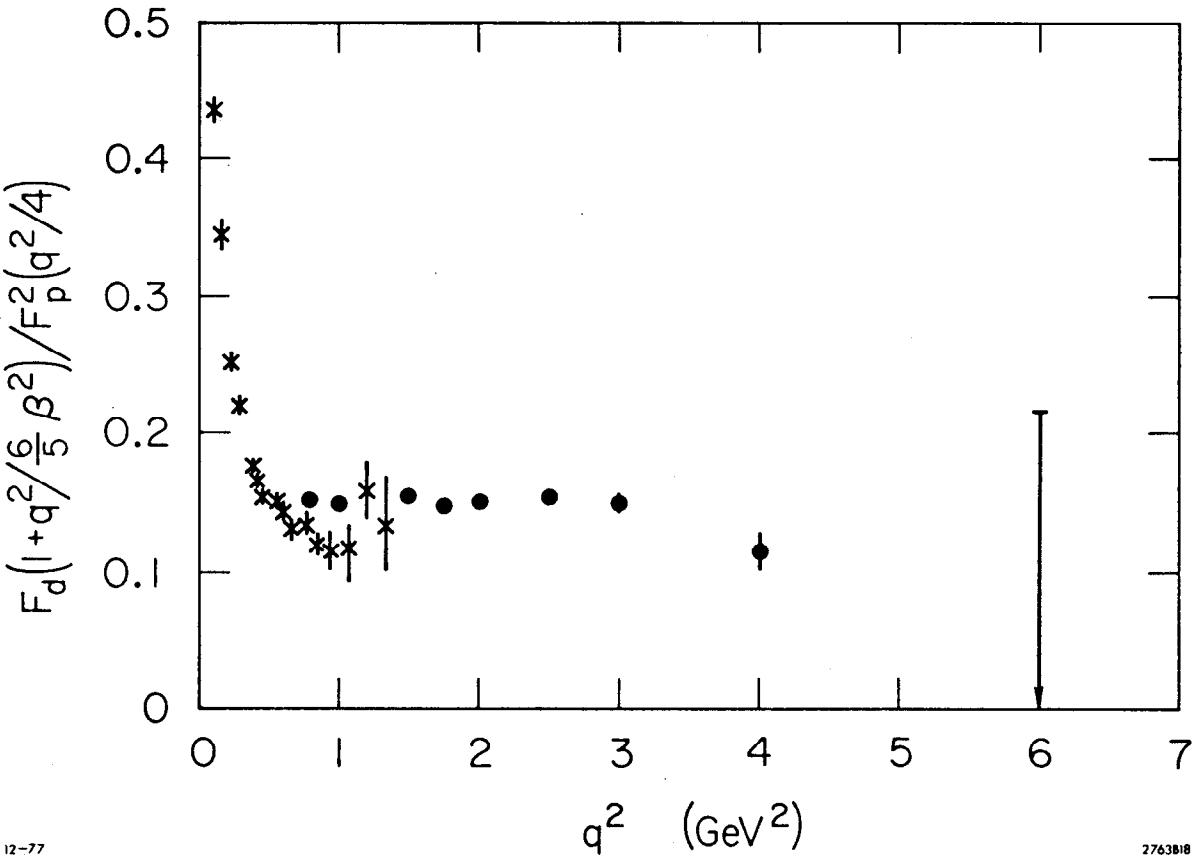
0.5
0.4
0.3
0.2
0.1
0
0
1
2
3
4
5
6
7
$F_d\left(1+q^2/\frac{6}{5}\beta^2\right)/F_p^2(q^2/4)$
q^2 (GeV^2)
12-77
2763B18

Fig. 15

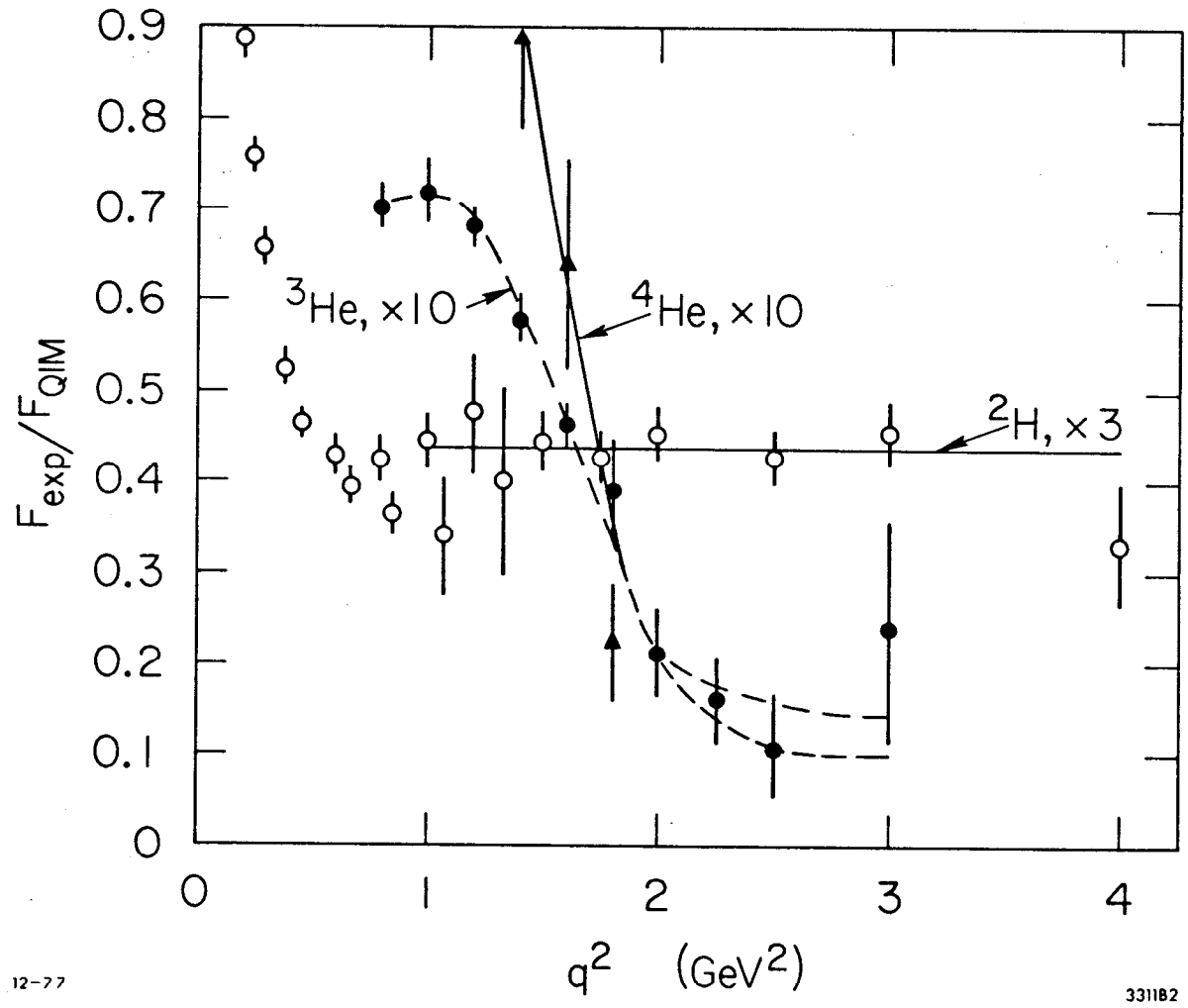
0.9
0.8
0.7
0.6
0.5
0.4
0.3
0.2
0.1
0
F_{exp}/F_{QIM}
^{3}He, ×10
^{4}He, ×10
^{2}H, ×3
0
1
2
3
4
q^2 (GeV^2)
12-77
3311B2

Fig. 16

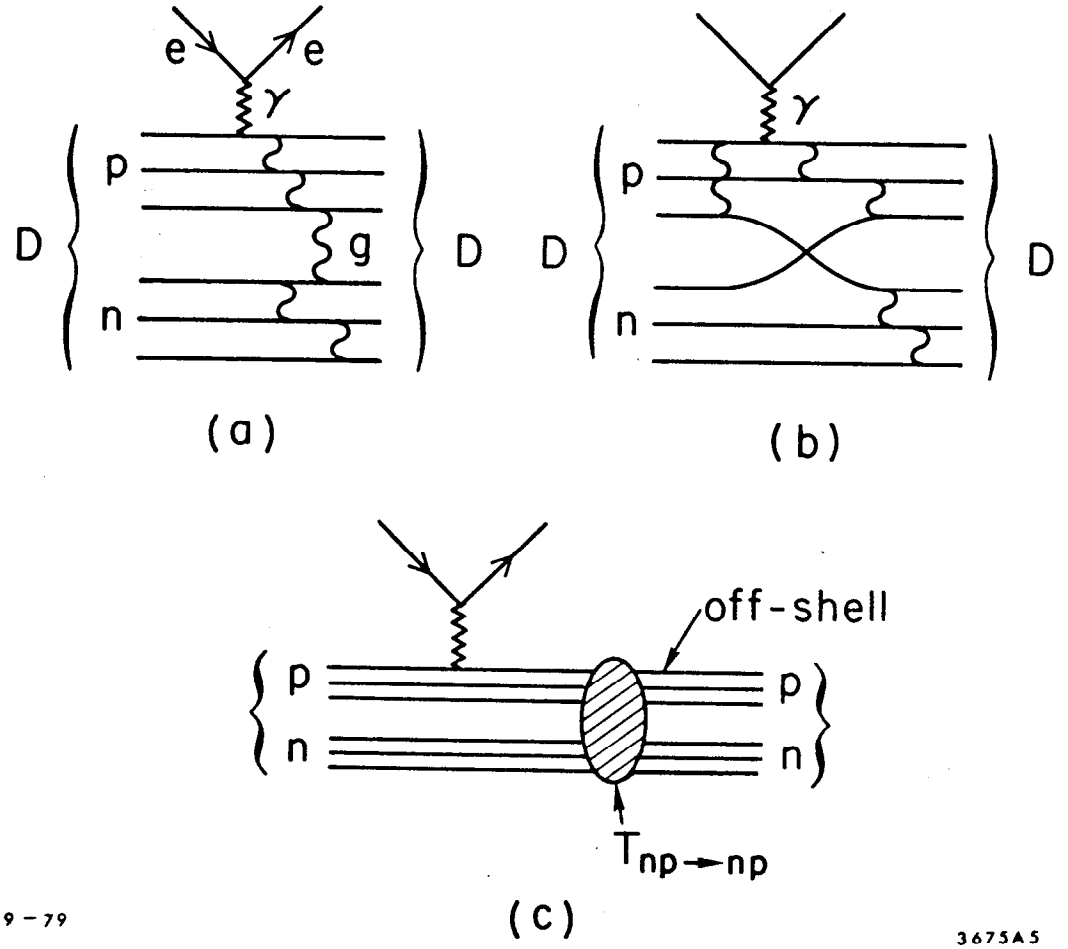

Fig. 17